

## Theoretical and Experimental Consideration of the Reactions between $V_xO_y^+$ and Ethylene

Dina R. Justes,<sup>†</sup> Roland Mitrić,<sup>‡</sup> Nelly A. Moore,<sup>†</sup> Vlasta Bonačić-Koutecký,<sup>\*,‡</sup> and A. Welford Castleman, Jr.<sup>\*,†</sup>

Contribution from the Departments of Chemistry and Physics, Pennsylvania State University, University Park, Pennsylvania 16802, and Humboldt Universität zu Berlin, Institut für Chemie, Brook-Taylor-Strasse 2, D-12489 Berlin, Germany

Received November 13, 2002; E-mail: vbk@chemie.hu-berlin.de; awc@psu.edu

**Abstract:** We present joint theoretical and experimental results which provide evidence for the selectivity of  $V_xO_y^+$  clusters in reactions toward ethylene due to the charge and different oxidation states of vanadium for different cluster sizes. Density functional calculations were performed on the reactions between  $V_xO_y^+$  and ethylene, allowing us to identify the structure–reactivity relationship and to corroborate the experimental results obtained by Castleman and co-workers (Zemski, K. A.; Justes, D. R.; Castleman, A. W., Jr. *J. Phys. Chem. A* **2001**, *105*, 10237). The lowest-energy structures for the  $V_2O_{2-6}^+$  and  $V_4O_{8-10}^+$  clusters and the  $V_2O_{3-6}^+-C_2H_4$  and  $V_4O_{10}^+-C_2H_4$  complexes, as well as the energetics for reactions between ethylene and  $V_2O_{4-6}^+$  and  $V_4O_{10}^+$  are presented here. The oxygen transfer reaction pathway was determined to be the most energetically favorable one available to  $V_2O_5^+$  and  $V_4O_{10}^+$  via a radical-cation mechanism. The association and replacement reaction pathways were found to be the optimal channels for  $V_2O_4^+$  and  $V_2O_6^+$ , respectively. These results are in agreement with the experimental results reported previously. Experiments were also conducted for the reactions between  $V_2O_5^+$  and ethylene to include an energetic analysis at increasing pressures. It was found that the addition of energy depleted the production of  $V_2O_4^+$ , confirming that a more involved reaction rather than a collisional process is responsible for the observed phenomenon. In this contribution we show that investigation of reactions involving gas-phase cationic vanadium oxide clusters with small hydrocarbons is suitable for the identification of reactive centers responsible for selectivity in heterogeneous catalysis.

### Introduction

The ability to selectively oxidize hydrocarbons is important to so many industrial processes,<sup>2,3</sup> and the development of catalysts that will efficiently accomplish this task continues to stimulate research in this field. The success in generating an effective catalyst, maximizing activity without sacrificing selectivity to the desired product, lies primarily in the greater understanding of the active sites responsible, and in identifying the mechanisms which govern the reaction. Without a better knowledge of the active sites responsible for effecting a particular reaction, information on a mechanism is also beyond comprehension. Elucidating the structure–reactivity relationship of surfaces is important in understanding catalytic selectivity and activity.<sup>4</sup> In view of the difficulty to identify specific active sites on a catalyst surface with the use of currently available

surface science techniques, alternative means of investigating the reaction mechanisms have been sought. It has been suggested that a metal oxide surface may be considered as a collection of metal oxide clusters of a variety of compositions and sizes,<sup>4,5</sup> and the study of gas-phase clusters has gained acceptance as one approach to model the active sites on catalytic surfaces.<sup>6</sup> As an example, molybdenum oxide surfaces may assume several spatial arrangements ranging in size from trimolybdates to hepta- and octamolybdates, depending on the experimental conditions.<sup>7</sup> Experiments on gas-phase clusters provide an appropriate environment to investigate the possible influences of composition, stoichiometry, charge and oxidation states, size, and degree of coordinative saturation on their reactivity. Studying the effect these characteristics have on the reactivity of the cluster provides insight into the nature of active sites responsible for a particular reaction. The guided ion beam mass spectrometer used in the studies reported herein is capable of mass-selecting metal oxide clusters of varying size and stoichiometry, providing information on the structure–reactivity relationship for the

<sup>†</sup> Departments of Chemistry and Physics, Pennsylvania State University.

<sup>‡</sup> Humboldt Universität zu Berlin, Institut für Chemie.

(1) Zemski, K. A.; Justes, D. R.; Castleman, Jr., A. W. *J. Phys. Chem. A* **2001**, *105*, 10237.

(2) Warren, B. K.; Oyama, S. T. *Heterogeneous Hydrocarbon Oxidation*; American Chemical Society: Washington, DC, 1996.

(3) Oyama, S. T.; Hightower, J. W. *Catalytic Selective Oxidation*; American Chemical Society: Washington, DC, 1993.

(4) Witko, M.; Hermann, K.; Tokarz, R. *J. Electron. Spectrosc. Relat. Phenom.* **1994**, *69*, 89.

(5) Muetterties, E. L. *Science* **1977**, *196*, 839.

(6) Lai, X.; Goodman, D. W. *J. Mol. Catal. A* **2000**, *162*, 33.

(7) Bielański, A.; Haber, J. *Oxygen in Catalysis*; Marcel Dekker: New York, 1991.

clusters under investigation, in particular when combined with the benefits afforded by the density functional methods reported here.

Another important issue that can be addressed through modeling active sites with ionic clusters is unraveling the role of charge and charge density. It has been proposed that OH and  $O^{2-}$  groups exist on  $\gamma$ - $Al_2O_3$  surfaces.<sup>7</sup> Also, Kung and co-workers have suggested that the active sites responsible for CO oxidation on a gold surface consist of a combination of  $Au^-$ —OH and metallic Au atoms.<sup>8</sup> Kiely and co-workers have proposed a cationic model involving  $Au^{x+}$  as an integral aspect of the mechanism for CO oxidation on a gold/iron oxide catalyst.<sup>9</sup> Significant relationships in reactivities have been observed between the gas and condensed phases. Zamaraev and co-workers have found similarities in the reactions of methanol with  $Mo_xO_y^+$  and those over heterogeneous catalysts.<sup>10</sup> Heiz, Landman et al. investigated experimentally and theoretically the reactivity of small gold clusters supported on magnesia and found  $Au_8$  to be a particularly reactive species to CO combustion.<sup>11</sup> The reactivity observed experimentally is likely due to an F-center defect which anchors the octamer to the surface.<sup>11</sup> Coadsorption of CO and  $O_2$  on small gold cluster anions has been also studied theoretically by Häkkinen and Landman<sup>12</sup> and experimentally by Bernhardt et al.<sup>13</sup> and Wallace and Whetten.<sup>14</sup> Theoretical methods, including charge sensitivity analysis<sup>15</sup> and ab initio<sup>16</sup> calculations, have been used to aid in the pursuit to identify and understand the active sites responsible for catalytic reactions.

In view of their ability to selectively oxidize hydrocarbons, vanadium oxides in particular are of interest to researchers.<sup>17–19</sup> Other research groups have actively pursued the active sites on vanadia catalysts, and some of these are reviewed in reference 20. The work reported in the present study was stimulated by the results obtained from the reactions between  $V_xO_y^+$  and ethylene and ethane carried out by the Castleman group at Penn State University.<sup>1</sup> The experiments showed significant and highly cluster-size-specific reaction pathways, which prompted further investigation to unravel the mechanism responsible for the observed phenomenon. Specifically, when  $(V_2O_5)_n^+$ , where  $n = 1–3$ , was reacted with ethane and ethylene,  $(V_2O_5)_{n-1}V_2O_4^+$  was identified as a very dominant reaction pathway. This reaction is outlined below using  $V_2O_5^+$  as the example although the reaction was also observed with  $V_4O_{10}^+$  and  $V_6O_{15}^+$ . Importantly, this reactive behavior attributable to oxygen transfer was not observed to any appreciable extent with

any other  $V_xO_y^+$  cluster.



The proposed product,  $C_2H_4O$ , is shown in parentheses since neutral species cannot be detected in the mass spectrometer used. The reaction shown above was proposed to be an oxygen transfer reaction from the metal oxide cluster to the hydrocarbon rather than oxygen loss because oxygen loss was not observed during low-energy collision-induced dissociation (CID) experiments conducted previously.<sup>21</sup> Rademann and Fielicke have investigated the interactions between the  $V_xO_y^+$  clusters with alkenes and alkanes and found a distinct reactivity of the  $(V_2O_5)_n^+$  toward the hydrocarbons studied.<sup>22</sup> In addition, Schwarz and co-workers performed studies on the reactivity of  $VO_2^+$  toward ethylene and found  $VO^+$  was produced, yielding acetaldehyde as the most likely neutral product.<sup>23</sup> To understand these observations, a combined experimental and theoretical effort was undertaken which allowed us to address the questions regarding the mechanism and energetic pathways for the oxygen transfer phenomenon observed for the  $(V_2O_5)_n^+$  clusters with ethylene.

In this work we present the results of density functional calculations, which provide key information on the structure–reactivity relationship for the reactions between the  $V_xO_y^+$  clusters and ethylene. The results include the optimized structures of the  $V_2O_{2-6}^+$  and  $V_4O_{8-10}^+$  clusters, of the  $V_2O_{3-6}^+ + C_2H_4$  and  $V_4O_{10}^+ + C_2H_4$  complexes and the reaction energetics for the reactions between the  $V_2O_{4-6}^+$  and  $V_4O_{10}^+$  clusters with ethylene including molecular dynamics (MD) simulations along the interesting reaction pathways. Our results allow for the proposal of a mechanism for the selective oxygen transfer due to the presence of the reactive centers for a given cluster size and stoichiometry, and they offer a clear explanation why different cluster sizes favor different processes. In light of the calculations conducted for this study, the issue whether the clusters, and hence the reactions themselves, involved interactions at well-defined thermal energies had become increasingly important. Therefore, an expanded experimental study of the size-specific reactions with additional energy was undertaken, whereby the products resulting from the  $V_2O_5^+$  and  $C_2H_4$  reactions were monitored at various energies and pressures. The experimental results reported here support the proposal that oxygen transfer is due to an exothermic reaction and not due to a collisional process resulting in oxygen loss from the cluster. In this contribution, after a brief description of computational and experimental methods, we present the results of the joint theoretical and experimental work and discussion.

## Computational Methods

Knowledge about the structural properties and energetics of neutral and anionic vanadium oxide clusters<sup>24</sup> as well as of cationic clusters,<sup>25</sup> is available from previous density functional studies. The findings are based on Becke's hybrid three parameter nonlocal exchange functional combined with the Lee–Yang–Parr gradient corrected correlation

- (8) Costello, C. K.; Kung, M. C.; Oh, H.-S.; Wang, Y.; Kung, H.-H. *Appl. Catal. A* **2002**, 232, 159.; Oh, H.-S.; Costello, C. K.; Cheung, C.; Kung, H. H.; Kung, M. C. *Stud. Surf. Sci. Catal.* **2001**, 139, 375.
- (9) Hodge, N. A.; Kiely, C. J.; Whyman, R.; Siddiqui, M. R. H.; Hutchings, G. J.; Pankhurst, Q. A.; Wagner, F. E.; Rajaram, R. R.; Golunski, S. E. *Catal. Today* **2002**, 72, 133.
- (10) Fialko, E. F.; Kikhtenko, A. V.; Goncharov, V. B.; Zamaraev, K. I. *J. Phys. Chem. B* **1997**, 101, 5772.
- (11) Sanchez, A.; Abbet, S.; Heiz, U.; Schneider, W.-D.; Häkkinen, H.; Barnett, R. N.; Landman, U. *J. Phys. Chem. A* **1999**, 103, 9573.
- (12) Häkkinen, H.; Landman, U. *J. Am. Chem. Soc.* **2001**, 123, 9704.
- (13) Hagen, J.; Socaciu, L. D.; Eljazyfer, M.; Heiz, U.; Bernhardt, T. M.; Wöste, L. *Phys. Chem. Chem. Phys.* **2002**, 4, 1707.
- (14) Wallace, W. T.; Whetten, R. L. *J. Am. Chem. Soc.* **2002**, 124, 7499.
- (15) Nalewajski, R. F.; Korchiwicz, J. *Comput. Chem.* **1995**, 19, 217.
- (16) Pacchioni, G.; Ferreri, A. M.; Giamello, E. *Chem. Phys. Lett.* **1996**, 255, 58.
- (17) Ruth, K.; Burch, R.; Kieffer, R. *J. Catal.* **1998**, 175, 27.
- (18) Escribano, V. S.; Busca, G.; Lorenzelli, V. *J. Phys. Chem.* **1990**, 94, 8945.
- (19) Oyama, S. T.; Somorjai, G. A. *J. Phys. Chem.* **1990**, 94, 5022.
- (20) Grzybowski-Swierkosz, B. *Appl. Catal. A* **1997**, 157, 409.

- (21) Bell, R. C.; Zemski, K. A.; Kerns, K. P.; Deng, H. T.; Castleman, A. W., Jr. *J. Phys. Chem. A* **1998**, 102, 1733.
- (22) Fielicke, A.; Rademann, K. *Phys. Chem. Chem. Phys.* **2002**, 4, 2621.
- (23) Harvey, J. N.; Diefenbach, M.; Schröder, D.; Schwarz, H. *Int. J. Mass Spectrom.* **1999**, 182/183, 85.
- (24) Vyboishchikov, S. F.; Sauer, J. *J. Phys. Chem. A* **2000**, 104, 10913.
- (25) Calatayud, M.; Andres, J.; Beltran, A. *J. Phys. Chem. A* **2001**, 105, 9760.

functional (B3LYP),<sup>26</sup> where either the all-electron triple- $\zeta$  valence plus polarization basis set (TZVP) developed by Ahlrichs and co-workers<sup>27</sup> or the standard double- $\zeta$  plus polarization AO basis set (DZP) was employed.<sup>25</sup> To determine the appropriate basis set for calculations undertaken in the present study, we employed both sets and compared the results with experimentally determined dissociation energies for  $VO^+$  and  $VO_2^+$ . Since the use of the DZP AO basis set does not provide reliable dissociation energies, we employ the TZVP AO basis sets throughout the work presented in this contribution. The calculated dissociation energies for  $VO^+$  and  $VO_2^+$  are 5.52 and 3.80 eV, using the TZVP AO basis sets, while the corresponding experimental values are  $D_e = 6.09 \pm 0.28$  and  $3.50 \pm 0.36$  eV, respectively.<sup>28</sup> Considering the large error bars which result when determining dissociation thresholds which also include the barrier, the calculated values are in acceptable agreement with the experimental findings. Gradient based minimization methods were used in order to determine structures; stationary points were characterized using vibrational frequency analysis. Transition states involved in the mechanism of the oxygen transfer reaction from  $V_2O_5^+$  and  $V_4O_{10}^+$  to ethylene have been optimized using the synchronous transit guided quasi-Newton (STQN) method developed by Schlegel and co-workers,<sup>29</sup> and barriers for the reaction steps were determined.<sup>30–32</sup>

The proposed oxygen transfer mechanism was studied and confirmed using ab initio molecular dynamics with forces calculated using the RI (resolution of identity)-DFT procedure<sup>32</sup> with the BLYP functional. To initiate the MD simulation, the activated complex of the  $V_2O_5^+$  cluster with ethylene was used. As initial conditions, the geometry of the stable complex was used, and initial velocities were generated by randomly distributing the energy corresponding to the stability of the complex among all internal degrees of freedom. MD simulations performed in this way enabled us to follow the reaction mechanism, and to verify the intermediates and reaction steps, involved in the oxygen transfer reaction.

## Experimental Section

The reactions between the group V metal oxide clusters,  $V_xO_y^+$ ,  $Nb_xO_y^+$ ,  $Ta_xO_y^+$  ( $x = 2–6$ ,  $y = 4–15$ ), and the C2 hydrocarbons were systematically investigated by the Castleman group at Penn State.<sup>1</sup> Among the products generated, one particular size selective reaction was observed between the  $(V_2O_3)_n^+$  ( $n = 1–3$ ) and ethylene which required further scrutiny. These experiments, which prompted the present study, were performed on a guided ion beam mass spectrometer coupled to a laser vaporization source described in detail elsewhere.<sup>28</sup> Briefly, the source consists of a metal rod ablated by the second harmonic of a Nd:YAG laser, and at a predetermined time, oxygen seeded in helium ( $\sim 8\%$ ) is pulsed over the source. The clusters are formed through plasma reactions and subsequently cooled using

supersonic expansion. This type of source creates a turbulent environment during cluster formation, which causes better thermalization of the clusters producing a cold ion beam.

The ion of interest is mass selected in the first quadrupole and focused into the octopole reaction cell through a set of electrostatic lenses. In this chamber, ethylene is introduced and maintained at a constant pressure while the energy of the octopole is increased incrementally ranging from 0 to 20 V, lab frame. These experiments were repeated for pressures 0.1 to 0.6 mTorr of ethylene in the collision cell. The products are then mass analyzed in the second quadrupole and detected using a channeltron electron multiplier.

## Results and Discussion

**Structures.** The optimized structures for the  $V_2O_{2–6}^+$  and the  $V_4O_{9,10}^+$  clusters are shown in Figure 1, where, atoms designated by an arrow indicate the location of the unpaired electron. In general agreement with the literature, the double-bridged structures for the  $V_2O_{2–6}^+$  are calculated to be the most stable structures.<sup>25,33</sup> For  $V_2O_4^+$ , two isomers with the terminal oxygen atoms occupying the trans and cis positions have been identified with an energy difference of 0.19 eV, the trans isomer being the lowest in energy. The  $V_2O_5^+$  structure contains an oxygen-centered radical, evidenced by the elongated bond, 1.78 Å compared to 1.56 Å for the other two terminal V–O bonds in the structure. Four isomers were found for the  $V_2O_6^+$  cluster: the lowest energy structure has two terminal V–O bonds and the  $O_2$  molecule is adsorbed to the cluster as a peroxide unit with the V–O bond lengths 1.92 and 1.97 Å and the O–O bond length 1.29 Å. Isomers II and III are the trans (II) and cis (III) configurations of the structures which have two terminal V–O bonds and one  $O_2$  molecule weakly adsorbed to the cluster by bonds with lengths 2.05 and 2.01 Å, respectively. Isomer III with the cis configuration of oxygen atoms is higher in energy by 0.17 eV than the trans isomer II. The fourth isomer, structure IV, shows four terminal V–O bonds and is higher in energy than the first isomer by 1.25 eV. The cationic structures of  $V_2O_{2–6}^+$  are closely related to the one obtained by Calatayud et al.<sup>25</sup> with the exceptions of  $V_2O_4^+$  and  $V_2O_6^+$ , in which case we found the trans isomers to have lower energies than the cis configurations and the  $O_2$  molecule in  $V_2O_6^+$  is bound as a peroxide unit. The structure for  $V_4O_8^+$ ,  $V_4O_9^+$ , and  $V_4O_{10}^+$  are shown in Figure 1f–h. They exhibit a cage structure similar to the one assumed by the  $P_4O_{10}$  molecule, suggested previously.<sup>34</sup> In the lowest-energy structure of  $V_4O_{10}^+$ , as in case of the  $V_2O_5^+$ , an oxygen-centered radical is present with a longer terminal V–O bond, 1.75 Å versus 1.55 Å for the other terminal V–O bonds, and the unpaired electron is on this oxygen atom, again designated by an arrow. The structures of the  $V_2O_{3–6}^+ - C_2H_4$  and  $V_4O_{10}^+ - C_2H_4$  complexes are shown in Figure 2.

The  $\Delta E$  values discussed below represent the calculated energies of formation for each complex. In the most stable complexes for  $V_2O_3^+ - C_2H_4$  and  $V_2O_4^+ - C_2H_4$ , the ethylene is bound directly to a three-coordinated vanadium atom with  $\Delta E = -0.26$  and  $-1.75$  eV, respectively. The complexes with ethylene bound directly to the terminal oxygen atom have in both cases considerably higher energies as shown in Figure 2. There are two isomers for the  $V_2O_5^+ - C_2H_4$  complex. One

(26) Becke, A. D.; *Phys. Rev. A* **1988**, 38, 3098.; Becke, A. D. *J. Chem. Phys.* **1993**, 98, 5648.; Lee, C.; Yang, W.; Parr, R. G. *Phys. Rev. B* **1998**, 58, 785.

(27) Schäfer, A.; Horn, H.; Ahlrichs, R. *J. Chem. Phys.* **1994**, 100, 5829.

(28) Bell, R. C.; Zemski, K. A.; Justes, D. R.; Castleman, A. W., Jr. *J. Chem. Phys.* **2001**, 114, 798.

(29) Peng, C.; Schlegel, H. B. *Isr. J. Chem.* **1993**, 33, 449.; Peng, C.; Ayala, P. Y.; Schlegel, H. B.; Frisch, M. J. *Comput. Chem.* **1995**, 16, 49.

(30) Ahlrichs, R.; Bär, M.; Häser, M.; Horn, H.; Kölmel, C. M. *Chem. Phys. Lett.* **1989**, 162, 165. Program TURBOMOLE.

(31) Frisch, M. J.; Trucks, G. W.; Schlegel, H. B.; Scuseria, G. E.; Robb, M. A.; Cheeseman, J. R.; Zakrzewski, V. G.; Montgomery, J. A., Jr.; Stratmann, R. E.; Burant, J. C.; Dapprich, S.; Millam, J. M.; Daniels, A. D.; Kudin, K. N.; Strain, M. C.; Farkas, O.; Tomasi, J.; Barone, V.; Cossi, M.; Cammi, R.; Mennucci, B.; Pomelli, C.; Adamo, C.; Clifford, S.; Ochterski, J.; Petersson, G. A.; Ayala, P. Y.; Cui, Q.; Morokuma, K.; Malick, D. K.; Rabuck, A. D.; Raghavachari, K.; Foresman, J. B.; Cioslowski, J.; Ortiz, J. V.; Stefanov, B. B.; Liu, G.; Liashenko, A.; Piskorz, P.; Komaromi, I.; Gomperts, R.; Martin, R. L.; Fox, D. J.; Keith, T.; Al-Laham, M. A.; Peng, C. Y.; Nanayakkara, A.; Gonzalez, C.; Challacombe, M.; Gill, P. M. W.; Johnson, B. G.; Chen, W.; Wong, M. W.; Andres, J. L.; Head-Gordon, M.; Replogle, E. S.; Pople, J. A. *Gaussian 98*, Revision A.7; Gaussian, Inc.: Pittsburgh, PA, 1998.

(32) Eichkorn, K.; Treutler, O.; Öhm, H.; Häser, M.; Ahlrichs, R. *Chem. Phys. Lett.* **1995**, 109, 47.

(33) Johnson, J. R. T.; Panas, I. *Inorg. Chem.* **2000**, 39, 3192.

(34) Berkowitz, J.; Chupka, W. A.; Inghram, M. G. *J. Chem. Phys.* **1957**, 27, 87; Brewer, L. *Chem. Rev.* **1953**, 52, 1.

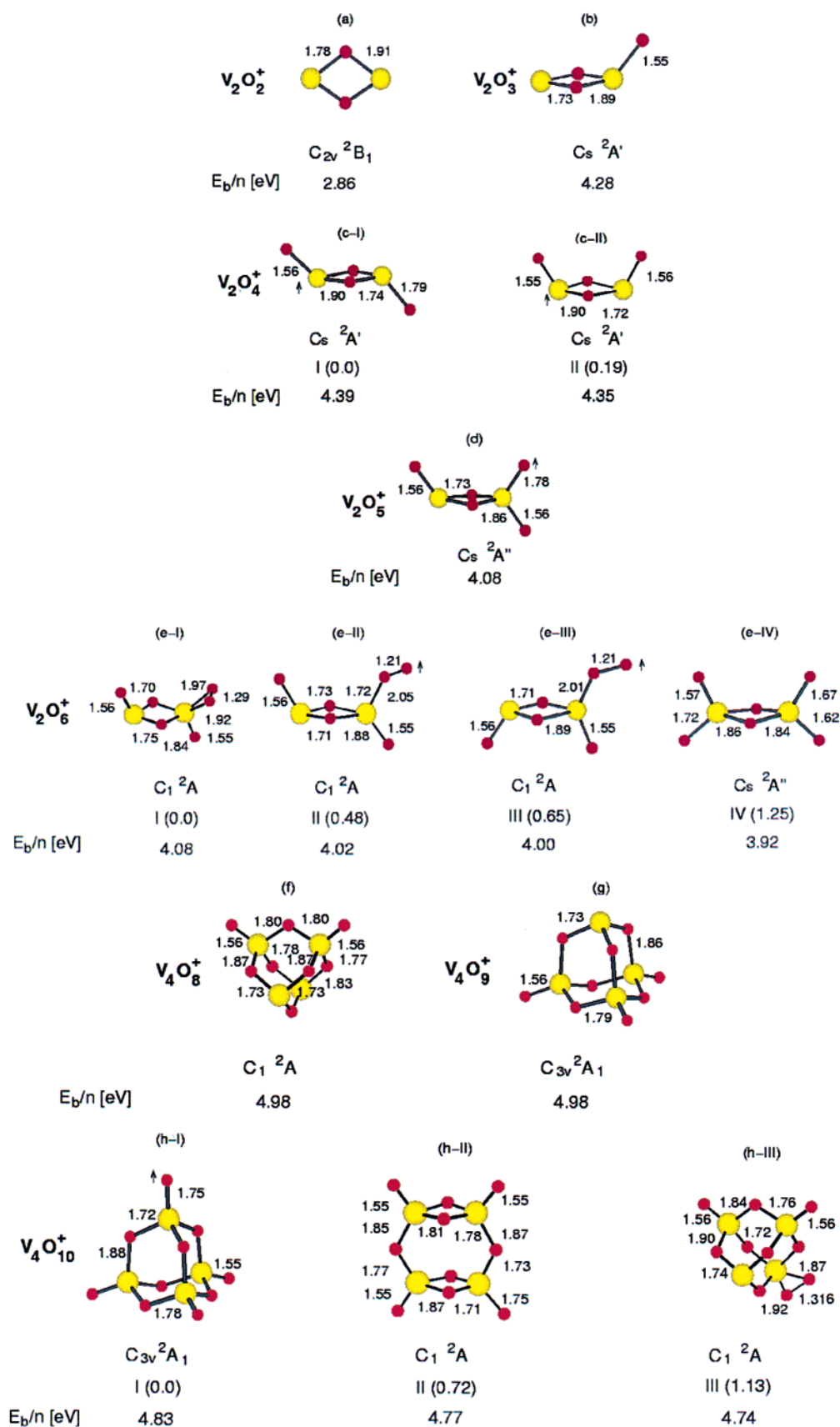


**Figure 1.** Structures for (a)  $V_2O_2^+$  (b)  $V_2O_3^+$ , (c-I) trans  $V_2O_4^+$ , (c-II) cis  $V_2O_4^+$ , (d)  $V_2O_5^+$ , (e-I) peroxo  $V_2O_6^+$ , (e-II) trans  $V_2O_6^+$ , (e-III) cis  $V_2O_6^+$ , (e-IV)  $V_2O_6^+$ , (f)  $V_4O_8^+$ , (g)  $V_4O_9^+$ , (h-I)  $V_4O_{10}^+$ , (h-II)  $V_4O_{10}^+$ , and (h-III)  $V_4O_{10}^+$  clusters. The energy differences in eV with respect to the most stable structures are given in round brackets. I–III label the energy sequence of the isomers. Labels of symmetry group and the ground electronic state are also given. Bond distances are in Å. Binding energies per atom (in eV) are defined as  $E_b/n = [E(V_xO_y^+) - E(V^+) - (x-1)E(V) - yE(O)]/(x+y)$ .



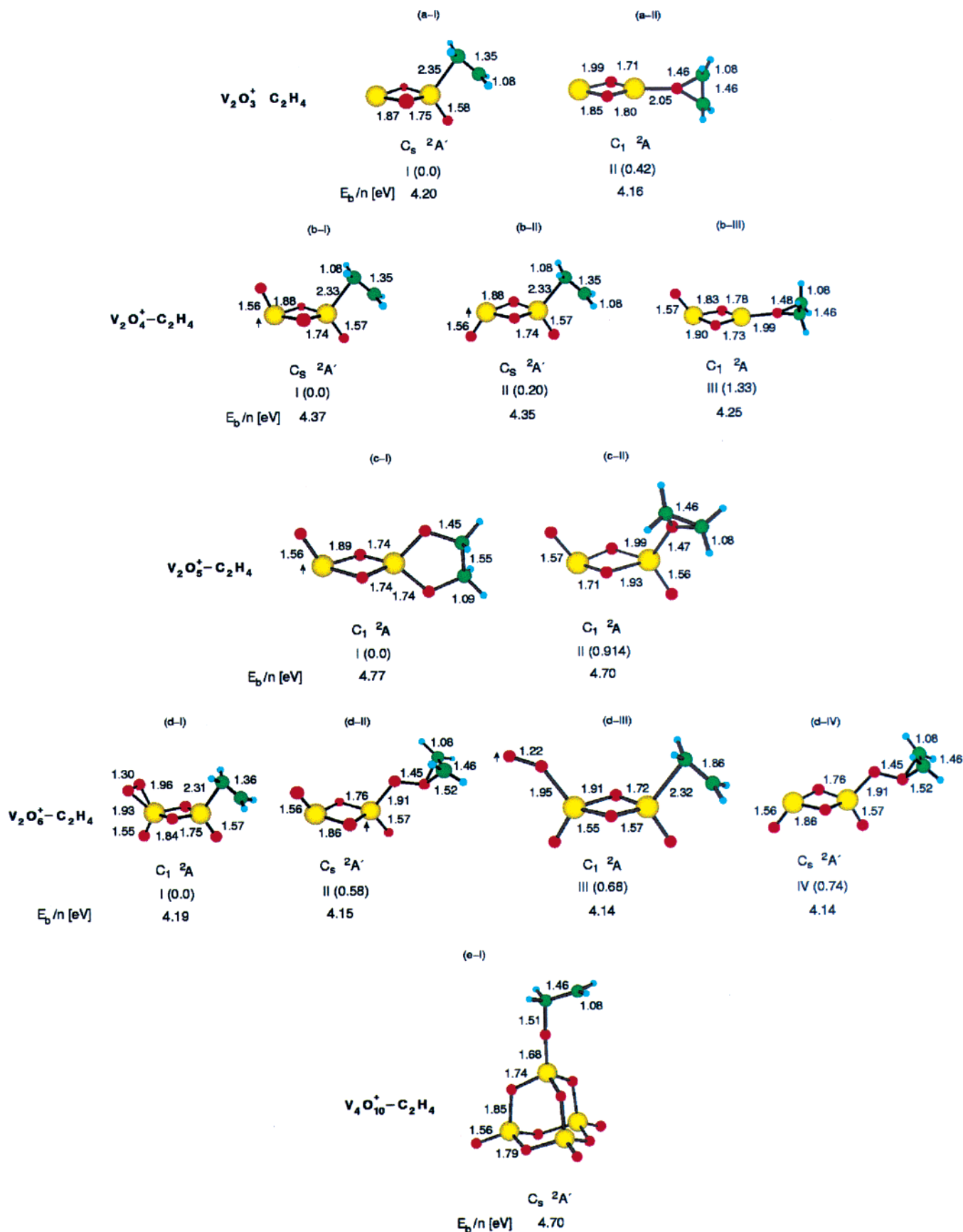
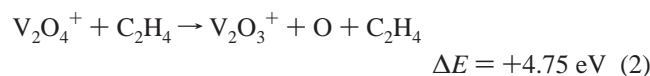


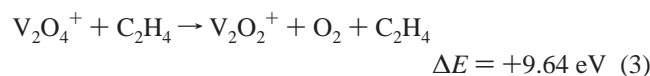
**Figure 2.** Structures for (a-I)  $V_2O_3^+ - C_2H_4$ , (a-II)  $V_2O_3^+ - C_2H_4$ , (b-I)  $V_2O_4^+ - C_2H_4$ , (b-II)  $V_2O_4^+ - C_2H_4$ , (b-III)  $V_2O_4^+ - C_2H_4$ , (c-I)  $V_2O_5^+ - C_2H_4$ , (c-II)  $V_2O_5^+ - C_2H_4$ , (d-I)  $V_2O_6^+ - C_2H_4$ , (d-II)  $V_2O_6^+ - C_2H_4$ , (d-III)  $V_2O_6^+ - C_2H_4$ , (d-IV)  $V_2O_6^+ - C_2H_4$  and (e)  $V_4O_{10}^+ - C_2H_4$  complexes. Binding energies per atom (in eV) are defined as  $E_b/n = [E(V_xO_y + C_2H_4) - E(V^+) - (x-1)E(V) - yE(O) - 2E(C) - 4E(H)]/(x+y+6)$ . For labels compare Figure 1.

structure depicts the ethylene bonding to the cluster through both terminal oxygen atoms,  $\Delta E = -4.44$  eV, and the second in which the ethylene is bound only to one oxygen atom,  $\Delta E = -3.53$  eV. The former structure has a lower energy than the latter.<sup>35</sup> There are four isomers for the  $V_2O_6^+-C_2H_4$  complex. In isomer I, the lowest-energy structure, the ethylene molecule is bound directly to the vanadium atom and the  $O_2$  molecule is adsorbed as a peroxo group to the other vanadium atom,  $\Delta E = -1.74$  eV. The second isomer (II) shows the ethylene bound to one oxygen atom of the adsorbed  $O_2$ ,  $\Delta E = -1.16$  eV. Isomer III differs from isomer I by the  $O_2$  molecule bound in the superoxo form,  $\Delta E = -1.06$  eV. Isomer IV is the trans configuration of isomer II. The differences in energy between isomer I and isomers II, III, and IV are 0.58, 0.68, and 0.74 eV, respectively. In the  $V_4O_{10}^+C_2H_4$  complex the ethylene binds to the oxygen atom with the radical center as shown in Figure 2.

**$V_2O_4^+$  Reactions.** The reactions between the  $V_2O_{4-6}^+$  clusters and ethylene are summarized in Table 1. Single oxygen atom loss from  $V_2O_4^+$  is not observed experimentally. The calculated energy for the single oxygen loss reaction for  $V_2O_4^+$  shows the reaction to be thermodynamically unfavorable with an energy of +4.75 eV shown in the following reaction.



Likewise, the energy for the reaction yielding molecular oxygen loss was determined to be +9.64 eV and, as expected, not seen during the experiment.

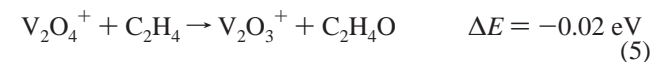


For the  $V_2O_4^+$  cluster, association is thermodynamically the most favorable pathway shown in reaction 4.



Experimentally, this is the only reaction channel observed for  $V_2O_4^+$  reactions with ethylene. The association product, although present under single-collision conditions, displays an increase in intensity with increasing ethylene pressure in the collision cell. This trend is expected due to a stabilizing effect of the third-body collisions which occur under multiple-collision conditions.

The oxygen transfer reaction for  $V_2O_4^+$  to yield  $C_2H_4O$  is marginally thermodynamically favorable with a calculated energy of  $-0.02$  eV, shown in reaction 5.



Although this reaction is slightly energetically favorable, it was not observed experimentally. This can be explained by the course the reaction takes. The oxygen transfer reaction occurs by first forming the association product between the cluster and the ethylene molecule. Then, to complete the oxygen transfer reaction pathway, a strong V–O bond must be broken, requiring 4.75 eV of energy. Considering that the association reaction

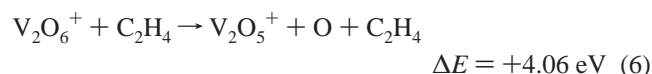
**Table 1.** Overview of the Important Theoretical and Experimental Reactions between  $V_xO_y^+$  and  $C_2H_4$

	$V_2O_1^+ + C_2H_4$	$V_2O_5^+ + C_2H_4$	$V_2O_6^+ + C_2H_4$	$V_4O_{10}^+ + C_2H_4$
<b>association:</b> calculated energy experiment	$V_2O_4^+ + C_2H_4 \rightarrow V_2O_4C_2H_4^+$ $\Delta E = -1.75$ eV only product observed	$V_2O_5^+ + C_2H_4 \rightarrow V_2O_5C_2H_4^+$ $\Delta E = -4.44$ eV minor product observed; excess energy released through fragmentation	$V_2O_6^+ + C_2H_4 \rightarrow V_2O_6C_2H_4^+$ $\Delta E = -1.74$ eV minor product observed; cleaving of V–O <sub>2</sub> bond, +0.92 eV likely	$V_4O_{10}^+ + C_2H_4 \rightarrow V_4O_{10}C_2H_4^+$ $\Delta E = -2.18$ eV minor product observed
<b>oxygen transfer:</b> calculated energy experiment	$V_2O_4^+ + C_2H_4 \rightarrow V_2O_3^+ + C_2H_4O$ $\Delta E = -0.02$ eV not observed; not breaking O–O bond too costly, 4.75 eV	$V_2O_5^+ + C_2H_4 \rightarrow V_2O_4^+ + C_2H_4O$ $\Delta E = -2.53$ eV dominant product observed; mechanism discussed in energetic profile	$V_2O_6^+ + C_2H_4 \rightarrow V_2O_5^+ + C_2H_4O$ $\Delta E = -0.71$ eV not observed; breaking O–O bond too costly, 4.06 eV	$V_4O_{10}^+ + C_2H_4 \rightarrow V_4O_9^+ + C_2H_4O$ $\Delta E = -1.36$ eV dominant product observed; mechanism discussed in energetic profile
<b>oxygen loss:</b> calculated energy experiment	$V_2O_4^+ + C_2H_4 \rightarrow V_2O_3^+ + C_2H_4 + O$ $\Delta E = +4.75$ eV not observed;	$V_2O_5^+ + C_2H_4 \rightarrow V_2O_4^+ + C_2H_4 + O$ $\Delta E = +2.24$ eV minor product observed; most likely oxygen transfer	$V_2O_6^+ + C_2H_4 \rightarrow V_2O_5^+ + C_2H_4 + O$ $\Delta E = +4.06$ eV not observed;	$V_4O_{10}^+ + C_2H_4 \rightarrow V_4O_9^+ + C_2H_4 + O$ $\Delta E = +2.75$ eV not observed; not energetically favourable
<b>molecular oxygen loss:</b> calculated energy experiment	$V_2O_4^+ + C_2H_4 \rightarrow V_2O_2^+ + C_2H_4 + O_2$ $\Delta E = +9.64$ eV not observed;	$V_2O_5^+ + C_2H_4 \rightarrow V_2O_3^+ + C_2H_4 + O_2$ $\Delta E = +1.78$ eV minor product observed; most likely formaldehyde formation	$V_2O_6^+ + C_2H_4 \rightarrow V_2O_4^+ + C_2H_4 + O_2$ $\Delta E = +1.09$ eV minor product; collisional process, observed during CID	
<b>replacement reaction:</b> calculated energy experiment		$V_2O_3^+ + C_2H_4 \rightarrow V_2O_3^+ + 2CH_2CO$ $\Delta E = -0.65$ eV	$V_2O_6^+ + C_2H_4 \rightarrow V_2O_4C_2H_4^+ + O_2$ $\Delta E = -0.66$ eV dominant product observed	

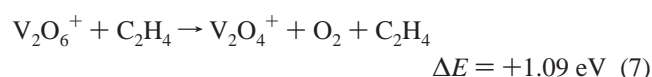
(35) Justes, D. R.; Castleman, A. W., Jr.; Mitrić, R.; Bonačić-Koutecký, V. *Eur. J. Phys. D.* In press.

only achieves a gain of 1.75 eV of energy, oxygen transfer is not energetically feasible. In addition, the ethylene molecule binds to a vanadium atom rather than to an oxygen atom, making the oxygen transfer reaction more complicated than simply breaking a V–O bond. Considering the steric issues and the energy barrier that must be overcome to break a V–O bond, it is very unlikely that this reaction pathway would be observed during the experiment. The theoretical calculations performed for the reactions between  $V_2O_4^+$  and ethylene provide an explanation for the reason that only one reaction pathway, namely association, is observed. Single and molecular oxygen losses are highly unfavorable energetically, and oxygen transfer has a barrier, which is too difficult to overcome under the experimental conditions.

**$V_2O_6^+$  Reactions.** The reaction for single oxygen loss from  $V_2O_6^+$  to produce  $V_2O_5^+$ , is not observed experimentally, and this can be explained by the calculated results. The single oxygen loss reaction is energetically unfavorable with  $\Delta E = +4.06$  eV as shown below.



The energy calculated for the molecular oxygen loss for  $V_2O_6^+$  was found to be +1.09 eV and is illustrated in the reaction below.



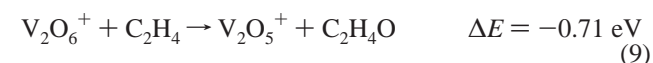
Even though the reaction is calculated to be endothermic, the loss of  $O_2$  from  $V_2O_6^+$ , which is observed during the experiment, is most likely the result of an ion-molecule impact. An alternative possibility is that the mass distribution is comprised of a large component of  $V_2O_6^+$  where  $O_2$  is weakly adsorbed to  $V_2O_4^+$ . During collision-induced dissociation experiments for  $V_2O_6^+$  interacting with xenon, molecular oxygen loss, forming  $V_2O_4^+$ , is observed at near thermal energies, implying that  $O_2$  is not strongly bound to the  $V_2O_4^+$  cluster.<sup>21</sup> This can also be seen from the structure of  $V_2O_6^+$  given in Figure 1e, which shows the  $O_2$  molecule bound to the cluster through bonds with lengths of 1.97 and 1.92 Å.

The association product for  $V_2O_6^+$  yielding  $V_2O_6^+-C_2H_4$  gains 1.74 eV of energy, shown below in reaction 8.



Association of ethylene to  $V_2O_6^+$  is observed experimentally, although it is only a minor pathway since a three-body mechanism is required for stabilization.

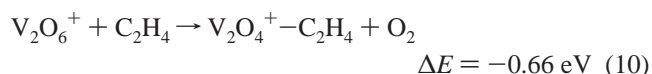
The oxygen transfer reaction for the  $V_2O_6^+$  cluster to yield  $C_2H_4O$  is thermodynamically favorable with an energy −0.71 eV, shown in reaction 9.



However, there is no experimental evidence for oxygen transfer to occur between the  $V_2O_6^+$  cluster and ethylene. As mentioned above, the association reaction produces 1.74 eV of energy for the complex. However, for the oxygen transfer reaction to occur, the V–O double bond must be broken in the first  $V_2O_6^+-C_2H_4$

isomer shown in Figure 2, requiring 4.70 eV, and this is evidently an insurmountable energy barrier for the reaction.

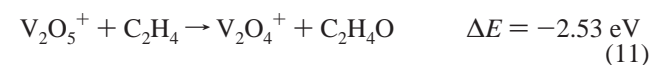
Experimentally, the  $V_2O_6^+$  undergoes a replacement reaction, yielding  $V_2O_4^+-C_2H_4$ , as the dominant product, illustrated below in reaction 10; yet it is slightly less energetically favorable than the oxygen transfer reaction (−0.66 eV versus −0.71 eV) shown above in reaction 9, although the energy difference may be within the limits of accuracy of the calculations. However, the replacement reaction does not require the cleavage of the strong O–O bond.



Although the association product for  $V_2O_6^+$  is energetically the most favorable channel (1.74 eV), as mentioned above, it is observed experimentally with a much weaker intensity than the replacement reaction. Again, due to the need for a third-body collision to stabilize the association complex, this result is in accordance with expectations. In the latter case it is possible that the amount of energy required to cleave the adsorbed  $O_2$  molecule from the complex, 1.09 eV, to yield  $V_2O_4^+-C_2H_4$ , is a relatively facile barrier to overcome, as indicated by MD simulations. Considering the amount of energy available to the complex and the ease with which this is accomplished for the  $V_2O_6^+$  cluster during CID experiments at near thermal energies, this possibility is very likely. In addition, at elevated reactant gas pressures, multiple collisions occur, increasing the likelihood of  $O_2$  loss and favoring the replacement reaction. The single oxygen loss and the oxygen transfer pathways are improbable due to energetic barriers involved in breaking the O–O bond. In conclusion, taking into account experimental conditions, as well as structural and energetic properties of involved species, we confirm that the replacement reaction, the most dominant pathway observed experimentally, is energetically the most viable option for the  $V_2O_6^+$  cluster.

**$V_2O_5^+$  Reactions.** Calculations were also performed on the possible reaction pathways for  $V_2O_5^+$  with ethylene.<sup>35</sup> The results are briefly summarized below. The association reaction forming  $V_2O_5^+-C_2H_4$  was determined to have two stable isomers, one formed through two terminal V–O bonds and the second through bonding to a single V–O terminal bond. The calculated energies were found to be energetically favorable by 4.44 and 3.53 eV for the respective isomers as discussed earlier. Atomic and molecular oxygen-loss pathways producing  $V_2O_4^+$  and  $V_2O_3^+$ , respectively, were calculated. The changes in energies were found to be thermodynamically unfavorable yielding +2.24 and +1.78 eV for atomic and molecular oxygen loss, respectively. Experimentally,  $V_2O_4^+$  and  $V_2O_3^+$  are observed products during the reactions with ethylene at thermal energies, yet neither is observed during CID at thermal energies. However, they are observed after the addition of 1–2 eV center-of-mass frame energy. These observations have led us to believe another mechanism must be responsible for each reaction.

Therefore, oxygen transfer is proposed to be responsible for the atomic and molecular losses observed during the experiments. Single oxygen transfer gives a  $\Delta E = -2.53$  eV to give  $V_2O_4^+$  and acetaldehyde shown in the reaction below.



Molecular oxygen transfer was a very minor product observed during the experiment and was found to have two possible mechanisms forming either ethene-diol,  $\Delta E = -1.05$  eV, or two formaldehyde molecules,  $\Delta E = -0.65$  eV. Despite the less favorable overall energy for producing two formaldehyde molecules, this reaction pathway is more likely to occur due to a high-energy barrier which makes formation of ethene-diol less probable.

It is important to note that the oxygen transfer phenomenon observed between the  $(V_2O_5)_n^+$  clusters and ethylene occur at both single- as well as multiple-collision conditions. Since the reactions occurred under single-collision conditions, there was no alternative mechanism available to the cluster to release the energy gained from the association reaction with ethylene.

To gain further insight into the course of the oxygen transfer reactions and to obtain additional confirmation about the proposed mechanism, ab initio MD simulations at constant energy corresponding to the microcanonical ensemble have been carried out. The results show that the association of ethylene to  $V_2O_5^+$  is followed by a very rapid (60–80 fs) hydrogen transfer from the carbon atom bound to oxygen toward the terminal carbon atom. After the hydrogen transfer has taken place, the V–O bond is broken within the next 100 fs, giving rise to the acetaldehyde and  $V_2O_4^+$  as the final products. In addition, the MD simulations also confirmed that the formation of two formaldehyde molecules and not the ethene-diol are products of the reaction giving  $V_2O_3^+$  as the minor product in the experiment. In view of the findings that oxygen atom loss can occur with sufficient collision energies with neutral atoms (Xe), we performed additional experiments to uncover the effect of systematically raising the energy of the reaction under conditions of constant selected pressures of ethylene within the reaction cell. The relative intensities of  $V_2O_5^+$ ,  $V_2O_4^+$ , and  $V_2O_3^+$  at varying energy are shown in Figure 3 as a function of increasing pressure, with the laboratory frame energy as the variable parameter. A common observation at each pressure in the branching ratio is the relative increase of  $V_2O_5^+$  and decrease of  $V_2O_4^+$  as the energy is increased incrementally. This indicates that as the energy of the reaction increases, the efficiency of the reaction decreases, i.e., less oxygen is being transferred to the ethylene. This is opposite to the trend that would arise if the oxygen atom loss were merely due to an unreactive, energetic CID process. The addition of energy has an effect of increasing the temperature of the system, thereby indicating this reaction system has a negative temperature dependence on the reaction efficiency. Barlow and co-workers studied the reaction between  $O_2^+$  and deuterated methanes and found conditions where, as the temperature increased, the rate coefficients decreased.<sup>36</sup> This phenomenon has been linked to the formation of a complex and the existence of an energy barrier to the forward reaction pathway that lies below the energy level of the reactants.<sup>36,37</sup> As can be seen in Figure 4a, the energy barrier of the transition state (TS) is lower in energy than that of the initial reactants and the proposed mechanism involves the formation of a complex. It has also been observed when the rate constant is significantly lower than the collision rate constant, a double-well exists, and the rates generally decrease

◇ - 5.1 V; □ - 10.1 V; △ - 15.1 V; ○ - 20.1 V

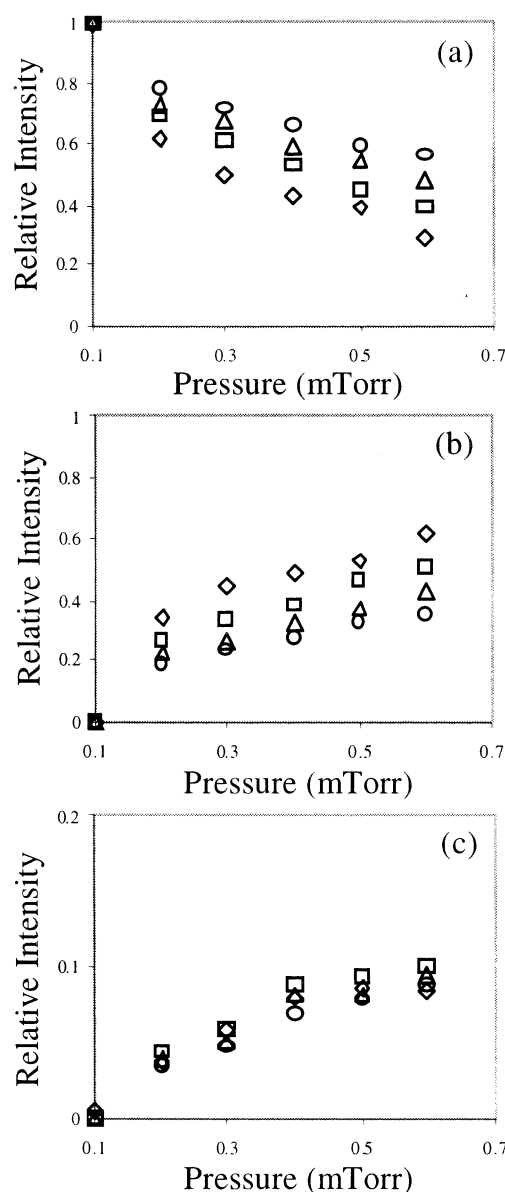


**Figure 3.** Branching ratios for the reaction between  $V_2O_5^+$  and  $C_2H_4$  as a function of pressure showing the relative intensities of (a)  $V_2O_5^+$ , (b)  $V_2O_4^+$ , and (c)  $V_2O_3^+$ . Each symbol represents a different energy, 5, 10, 15, and 20 V.

with increasing temperature up to a certain point.<sup>38</sup> The collision rate for the reaction between  $V_2O_5^+$  and ethylene should be somewhat higher than  $10^{-9} \text{ cm}^3/\text{s}$  and our preliminary investigation into the rate constants for this reaction shows the value to be considerably lower than this. It has been shown that negative temperature dependencies do occur for slow bimolecular exchange reactions which do not possess a positive activation energy in the forward direction toward the production of the association complex.<sup>38,39</sup> That such a situation arises in the present reaction can be seen from the energetic profile in Figure 4a; the initial step in the oxygen transfer reaction is the formation of a very stable association complex without an activation barrier to overcome.

(36) Barlow, S. E.; Van Doren, J. M.; DePuy, C. H.; Bierbaum, V. M.; Dotan, I.; Ferguson, E. E.; Adams, N. G.; Smith, D.; Rowe, B. R.; Marquette, J. B.; Dupeyrat, G.; Durup-Ferguson, M. *J. Chem. Phys.* **1986**, *85*, 3851.  
(37) Olmstead, W. N.; Brauman, J. I. *J. Am. Chem. Soc.* **1977**, *99*, 4219.

(38) Lindinger, W.; Fehsenfeld, F. C.; Schmeltekopf, A. L.; Ferguson, E. E. *J. Geophys. Res.* **1974**, *79*, 4753.

(39) Meot-ner, M. *Gas-Phase Ion Chem.* **1979**, *1*, 197.



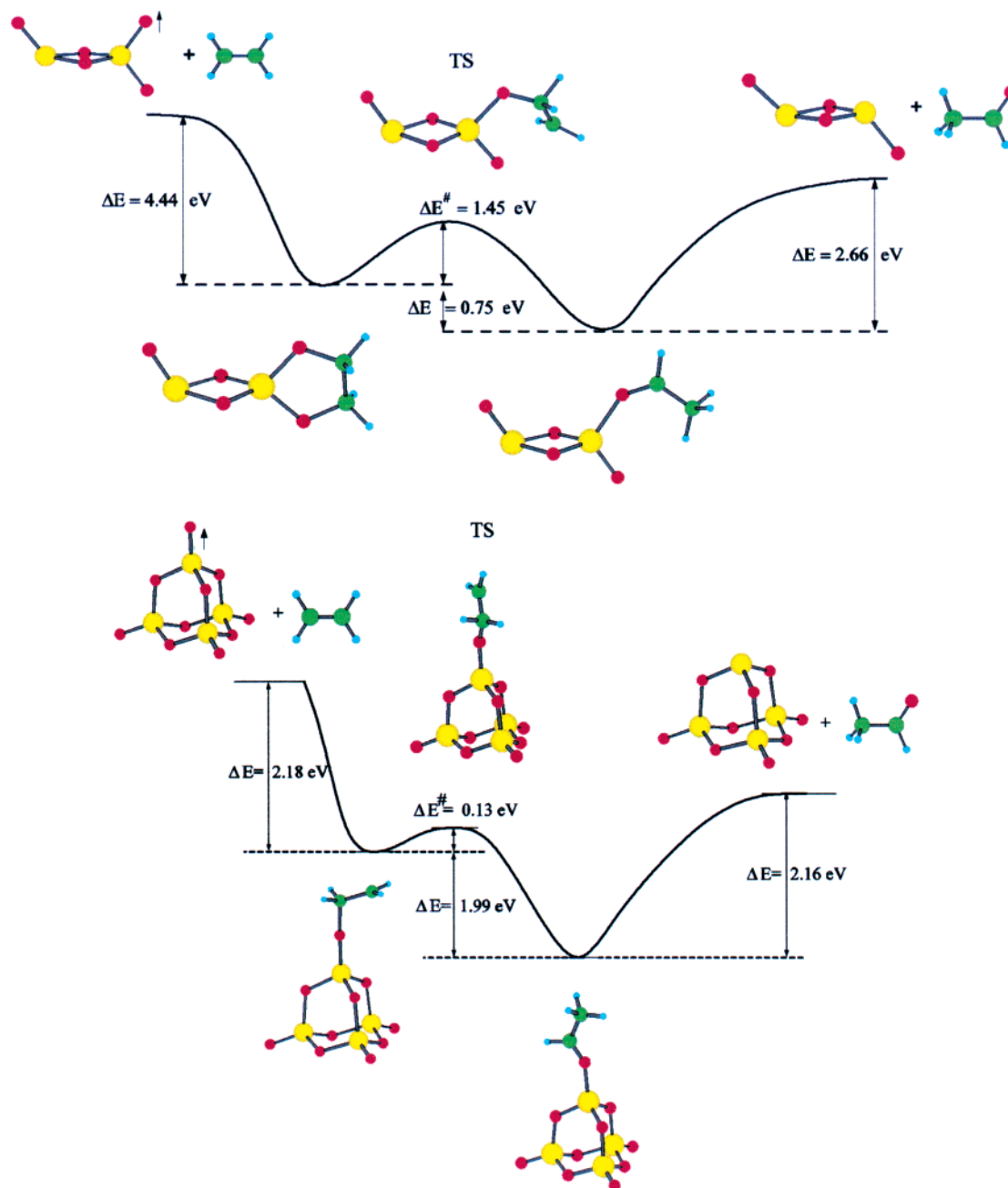


**Figure 4.** Energetic profile for the reaction between (a)  $V_2O_5^+$  and (b)  $V_4O_{10}^+$  and  $C_2H_4$ .

The parallels discussed above between our results and other kinetic studies on reactions involving intermediate complexes and transition states provides further support for our proposed mechanism for the oxygen transfer reaction to  $C_2H_4$  from  $V_2O_5^+$ .

It is also important to note that if the process occurring between  $V_2O_5^+$  and  $C_2H_4$  was a simple collisional process, resulting in the production of  $V_2O_4^+$ , O and  $C_2H_4$ , the intensity of  $V_2O_4^+$  would increase, not decrease, as energy is added, as would occur in the case of a collision-induced dissociation reaction. This energetic analysis is also further evidence that the vanadium oxide cluster ions are thermalized during their reactions in the collision cell. Another possibility to consider is whether further reactions are occurring to yield  $V_2O_3^+$ . However, as can be seen in Figure 3c, the intensity of  $V_2O_3^+$  does not increase over the energy range studied, and no other

reaction products are observed in the mass spectra. The reverse reaction for the  $V_2O_3^+$  reaction is unlikely since two formaldehyde molecules would need to be present for the reverse reaction to take place, and this is statistically highly improbable. Also, similar to the oxygen transfer possibility discussed above, further reactions would not account for the rise in  $V_2O_5^+$  intensity observed as the energy in the collision cell is increased.

**$V_4O_{10}^+$  Reactions.** Considering that the oxygen transfer reaction occurred only for clusters with the stoichiometry,  $(V_2O_5)_n^+$  with  $n = 1-3$ , the question remained whether a common structural element is present in each of the three clusters. By using density functional theory, it was determined that  $V_2O_5^+$  was an oxygen-centered radical, and after additional calculations were performed, it was found that  $V_4O_{10}^+$  also had this characteristic. There is an elongated terminal V–O bond and an unpaired electron localized at the oxygen atom common

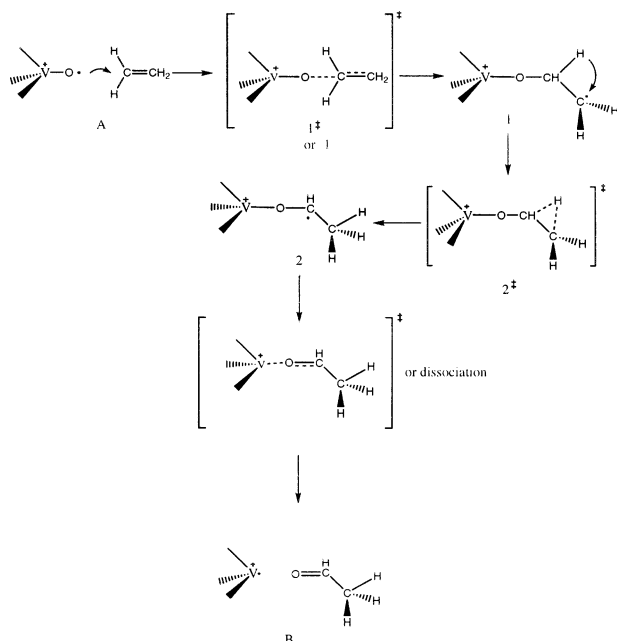
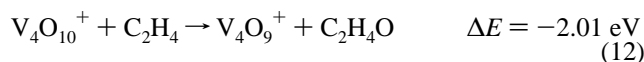


**Figure 5.** General mechanism for the reaction between  $(V_2O_5)_n^+$ ,  $n=1,2$  and  $C_2H_4$ .

to both  $V_2O_5^+$  and  $V_4O_{10}^+$ , designated by an arrow as seen in Figure 1d and 1h. The oxygen transfer reaction between  $V_4O_{10}^+$  and ethylene is shown below.



Similar to the reaction for  $V_2O_5^+$ , this reaction is also thermodynamically favorable. The energetic profile for the reaction is shown in Figure 4b. The pathway depicted in Figure 4b for the reaction between  $V_4O_{10}^+$  and ethylene is very similar to the one just described for the reaction with  $V_2O_5^+$  shown in Figure 4a.<sup>34</sup> However, unlike the  $V_2O_5^+$  cluster binding ethylene to two oxygen atoms, the  $V_4O_{10}^+$  cluster initially binds the ethylene molecule through a single oxygen atom. This is due to the terminal oxygen atoms being too far apart in the  $V_4O_{10}^+$  cluster for the ethylene to bind two terminal O atoms (cf. Figure 2). As can be seen in the energetic profile for the reaction between  $V_4O_{10}^+$  and ethylene in Figure 4b, the transfer of the hydrogen from the oxygen-bound carbon to the second carbon is lower in energy than the activated complex by 1.99 eV. The V–O is then cleaved, separating the  $C_2H_4O$  from the  $V_4O_9^+$  cluster. It should be pointed out that a weak molecular oxygen loss channel was also observed experimentally, giving  $V_4O_8^+$  as a product. This, however cannot be due to the most stable structure of  $V_4O_{10}^+$ , as determined through DFT calculations, but to the higher-energy isomer (cf. Figure 1). It is possible that in the cluster beam a small amount of  $V_4O_8^+$  with adsorbed molecular oxygen, which can be easily released at thermal energies, is present. Experimentally, the production of  $V_4O_8^+$  from  $V_4O_{10}^+$  is most likely a collisional process since this reaction is observed during collision induced dissociation experiments conducted previously in our laboratory.<sup>21</sup> In support of this, Asmis et al. observed the  $V_4O_8^+$  fragment when  $V_4O_{10}^+$  was photodissociated, supporting the  $V_4O_8^+-O_2$  structure of  $V_4O_{10}^+$ .<sup>40</sup>

**Oxygen Transfer Radical-Cation Mechanism.** The energetic profiles for the oxygen transfer reactions for  $V_2O_5^+$  and

$V_4O_{10}^+$  are shown in Figure 4, a and b, respectively. They show the proposed pathways, which the reactions between  $V_2O_5^+$  and  $V_4O_{10}^+$  with ethylene are most likely to take. The general mechanism for this reaction is proposed in Figure 5. The mechanism begins with the formation of a single bond between the first carbon atom of the ethylene and the oxygen atom. The radical, initially located on the oxygen atom, is transferred to the second carbon atom in the ethylene molecule. The radical is then shifted from the second carbon atom to the first carbon atom by hydrogen transfer from the first carbon to the second carbon. Dissociation of the  $C_2H_4O$  product then occurs, leaving the vanadium atom, which had been bound to the oxygen atom with the radical center. Comparison of the reaction pathway for  $V_2O_5^+$  and  $V_4O_{10}^+$  shows that reaction intermediates have very similar relative stabilities with respect to the reactants and the products, reflecting common structural properties and the generality of the proposed mechanism.

## Conclusions

In conclusion, the structure–reactivity relationship for  $V_xO_y^+$  clusters toward ethylene has been clearly identified. An overview of our theoretical and experimental results is given in Table 1. The radical center located at one of the peripheral O atoms in  $V_2O_5^+$  and  $V_4O_{10}^+$  is responsible for the observed oxygen transfer in the framework of radical-cation mechanism. In addition to the structural properties, the strength of the bond between the transition metal atom and the oxygen atom also plays an important role in the oxygen transfer. For example, our preliminary calculations indicate that despite the common structural properties of  $Nb_2O_5^+$  and  $V_2O_5^+$ , oxygen transfer from  $Nb_2O_5^+$  to ethylene is observed to a considerably lower extent, due to the stronger Nb–O bonding.

Our experimental and theoretical results provide evidence for the selectivity of the  $V_xO_y^+$  clusters due to the charge as well as the capability of vanadium to assume different oxidation states for different cluster sizes. In the case of  $(V_2O_5)_n^+$ ,  $n = 1,2$ , the oxygen atom can be reversibly bound and released promoting catalytic oxidation of hydrocarbons, providing evidence that gas-phase clusters can serve as well suited prototypes for identification of reactive centers. In fact, the active sites identified as being responsible for oxidation are in agreement with indirect experimental findings of active sites on vanadia/titania surface,<sup>41</sup> which were used to explain the formation of products such as acetaldehyde and formaldehyde. This illustrates that the study of reactions involving gas-phase cationic vanadium oxide clusters and small hydrocarbons is suitable for identification of reactive centers responsible for selectivity in heterogeneous catalysis.

There have been several condensed phase studies performed on the oxidation of ethane and ethylene over vanadia catalysts.<sup>18–20,42–45</sup> Acetaldehyde was an observed oxidation product

- (40) Asmis, K. R.; Brümmer, M.; Kaposta, C.; Santambrogio, G.; von Helden, G.; Meijer, G.; Rademann, K.; Wöste, L. *Phys. Chem. Chem. Phys.* **2002**, *4*, 1101.
- (41) Luan, Z.; Meloni, P. A.; Czernuszewicz, R. S.; Kevan, L. J. *Phys. Chem. B* **1997**, *101*, 9046.
- (42) Oyama, S. T.; Middlebrook, A. M.; Somorjai, G. A. *J. Phys. Chem.* **1990**, *94*, 5029.
- (43) Linke, D.; Wolf, D.; Baerns, M.; Timpe, O.; Schlögl, R.; Zeyss, S.; Dingerdisen, U. *J. Catal.* **2002**, *205*, 16.
- (44) Argyle, M. D.; Chen, K.; Bell, A. T.; Iglesia, E. *J. Phys. Chem. B* **2002**, *106*, 5421.
- (45) Otsuka, K.; Urugami, Y.; Hatano, M. *Catal. Today* **1992**, *13*, 667.

of ethane and ethylene over vanadia/silica catalysts.<sup>42</sup> In addition, ethylene is a significant product of the oxidation of ethane over vanadia catalysts<sup>43,44</sup> and is proposed to be one of the pathways ultimately yielding acetaldehyde.<sup>35</sup> Finally, Otsuka and co-workers were able to achieve a higher yield of acetaldehyde from the partial oxidation of ethane, which they attribute to an increased number of the active sites they believe are responsible for the reaction.<sup>45</sup> This shows that a greater understanding of the active sites which facilitate certain catalytic

processes can in fact lead to custom-designed catalysts for specific purposes.

**Acknowledgment.** We acknowledge the National Science Foundation, Grant No. CHE-99-06341 for financial support of the experimental work reported herein and for the collaboration with the Bonačić-Koutecký research group. Helpful discussions with Eldon E. Ferguson are gratefully acknowledged.

JA021349K